Gearless Micro Hydropower Plant for Small Water-Course

Yury Dementyev[1], Roman Kuzmin[2], Aleksandr Serikov[2], Viktor Suzdorf[2], Kirill Negodin[1], Istvan Vajda[3]

[1]Tomsk Polytechnic University, Institute of Power Engineering, av. Lenina 30, 634050 Tomsk, Russian Federation , e-mail dementev@tpu.ru; knn1@tpu.ru

[2]Komsomolsk-na-Amure State Technical University, Electrotechnical Faculty, av. Lenina 27, 681013 Komsomolsk-na-Amure, Khabarovsk region, Russian Federation, e-mail epapu@knastu.ru; kepapu@knastu.ru; em@knastu.ru

[3]Óbuda University, Kandó Kálmán Polytechnic, Bécsi út 96/b, 1034 Budapest, Hungary, e-mail vajda@uni-obuda.hu

Abstract: The paper focuses on problem of development of autonomous power-supply systems based on micro hydropower plants, which are using small watercourse power. The design and development of such systems is influenced by a number of conflicting objectives. The power source has to generate ac voltage with steady-state magnitude and frequency and, at the same time, it has to be fairly simple and inexpensive. One of the future-proof designs that provides fulfillment of the above mentioned requirements is a gearless micro hydropower plant with a combined impeller of axial-flow turbine and an electric arc-shape inductor generator. The authors have identified how geometrical parameters of the arc-shape inductor generator influences the machine operation factors. In addition, they have found that the air gap impacts the ripple factor significantly. Finally the paper shows functional dependence of the slot chamfer factor on chamfer angle, which simplifies the problem of choosing reasonable, in terms of efficiency, design parameters of the generator for the micro hydropower plant

Keywords: micro hydropower plant; arc-shape inductor generator; form factor; design solutions; parameter optimization; ripple factor; chamfer angle

1 Introduction

During the 18th, 19th and the first half of the 20th Century, water wheels were important hydraulic energy converters. It is estimated that in England 25,000-30,000 wheels were in operation around 1850; in Germany 33,500 water wheels were recorded as late as 1925. Today, only very few water wheels are still in use.

Low power hydropower is seldom exploited since cost-effective energy converters for these conditions are not available [1]. Design of autonomous power-supply systems for lowland rivers with small watercourse power is carried out by solving the whole range of conflicting problems. The power source has to generate ac voltage with steady-state magnitude and frequency and, at the same time, it has to be fairly simple and inexpensive. One of future-proof designs that meets the above-mentioned requirements is gearless micro hydropower plant with combined impeller of axial-flow turbine and electric arc-shape inductor generator [1]. An advantage of propeller-type axial flow turbines is maximal specific speed for low heads, which allows for the development of a gearless micro hydropower plant. Hydroturbine in a river with low flow rate is placed on floats in order to be able to adjust the depth of the impeller immersion into water, so it does not have negative impact on the environment, including on spawning rivers. Thereby, the problem of designing electric power supply systems based on gearless micro hydropower plants for lowland rivers is topical [2].

Simplified design of hydroturbine in lowland river is shown in Fig. 1.

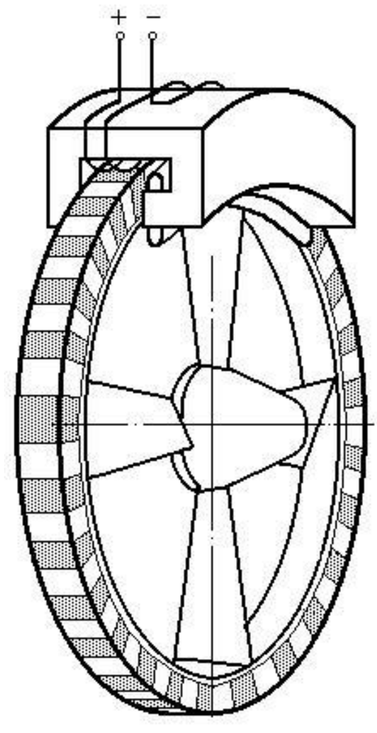

Figure 1

Hydroturbine for lowland river

Simulation of such a complex technical object as a micro hydropower plant is carried out based on generally accepted assumptions. The simulation outcomes should indicate characteristics of efficiency and other parameters of the device performance quality. Initial parameters that determine all the simulation factors are the turbine diameter, blade angle, water course velocity [3].

Simulation model studies have shown the main relationships of the design parameters on parameters of the water course. Functions shown in Fig. 2 compose 3D characteristic «Power of hydroturbine, P_G – water course velocity V_w - turbine wheel diameter D_w».

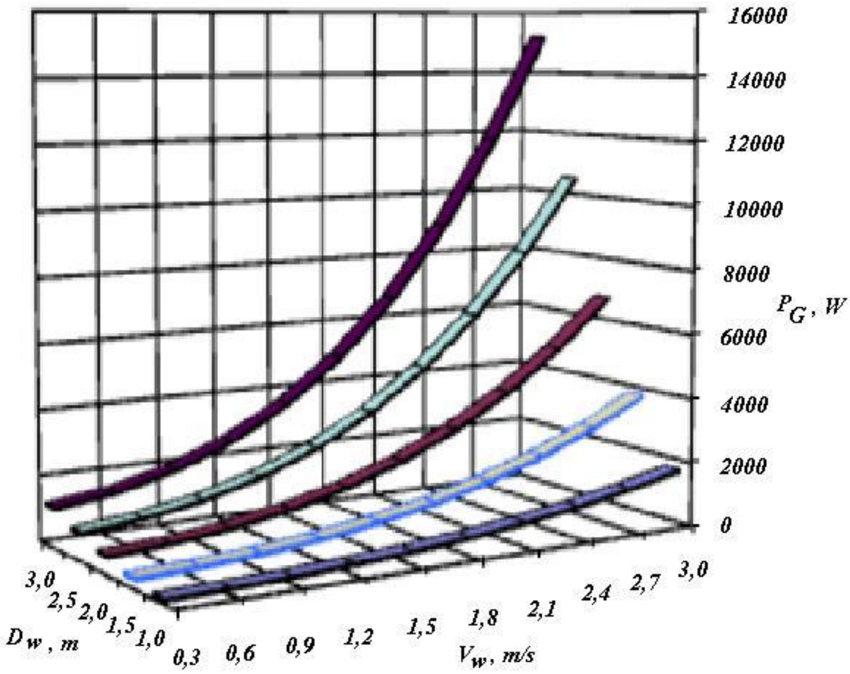

Figure 2
Functions «Power of hydroturbine – water course velocity - turbine wheel diameter»

2 Design and Calculation of the Arc-Shape Generator

The source of electric energy is a generator of special developed design, which determines all other parameters of the system. Therefore, it is important to predetermine static and dynamic characteristics of the source based on the generator in the designing phase [3]. So, we need to develop adequate mathematical model of an electric arc-shape inductor generator of a special developed arc-shape design.

Structure features of the inductor generator with an arc-shape stator influence on the form of magnetic field in the air gap demands corresponding analysis to determine dependencies of parameters of the generator and the field harmonic composition as well as the losses on higher harmonics.

Magnetic induction distribution in the air gap of synchronous electric arc-shape inductor generator with electromagnetic excitation is described by an equation set of the stationary magnetic field [4]. One of main approaches to its solution is finite element method (FEM).

Constructively the magnetic core is made of laminations, that is why at the stage of mathematical description of the generator magnetic circuit it is convenient to use the projections of magnetic permeability on two axes (Y,X) that correspond to longitudinal and transversal lines of the iron rolling.

Considering non-saturated magnetic circuit of the generator, the following equations [5] can be used:

- Magnetic permeability in Y-axis (along rolled sheet), H/m, is determined in terms of formula:

$$\mu_Y = \mu_{ir} \cdot K_L ,$$

where μ_{ir} is relative permeability of iron; K_L is lamination factor.

- Magnetic permeability in X-axis (across rolled sheet), H/m, is determined in terms of formula:

$$\mu_X = \frac{(2 - K_L) \cdot \Delta_{ir}}{\frac{\Delta_{ir}}{\mu_{ir}} + \frac{\Delta_{ir} \cdot (1 - K_L)}{\mu^{\ddot{e}}{}_0}} ,$$

where Δ_{ir} is thickness of rolled sheet, m;

$\mu^{\ddot{e}}{}_{ir} = 1$ is value of relative permeability of iron.

- Magnetizing force in the air gap of the generator is determined by:

$$F_\delta = \frac{B_\delta}{\mu_0} \cdot \delta ,$$

where δ is value of air gap, m.

- Magnetic potential difference in the air gap between stator and rotor is given by:

$$U_m = F_\delta .$$

Boundary conditions, which are taken into account to solve the field problem, are the following [4] :

- boundary conditions of the first kind on external (upper and lower) borders of the simulated area (homogeneous) (see Fig. 3)are given by:

$$U_{m\lfloor B \rfloor} = const\,.$$

- boundary conditions of the second kind on external (left and right) borders of the simulated area (see Fig. 3) are determined in terms of:

$$\left.\frac{\partial U_m}{\partial n}\right|_{\lfloor B \rfloor} = 0\,.$$

The last condition is true, when moving away the borders of the area for a considerable distance from the field source.

It is necessary to maintain the continuity condition of magnetic scalar potential and equality of normal and tangential derivatives on the interfacial area. In finite element method these conditions are met automatically. Computational area of the magnetic field studies with boundary conditions is shown in Fig. 3.

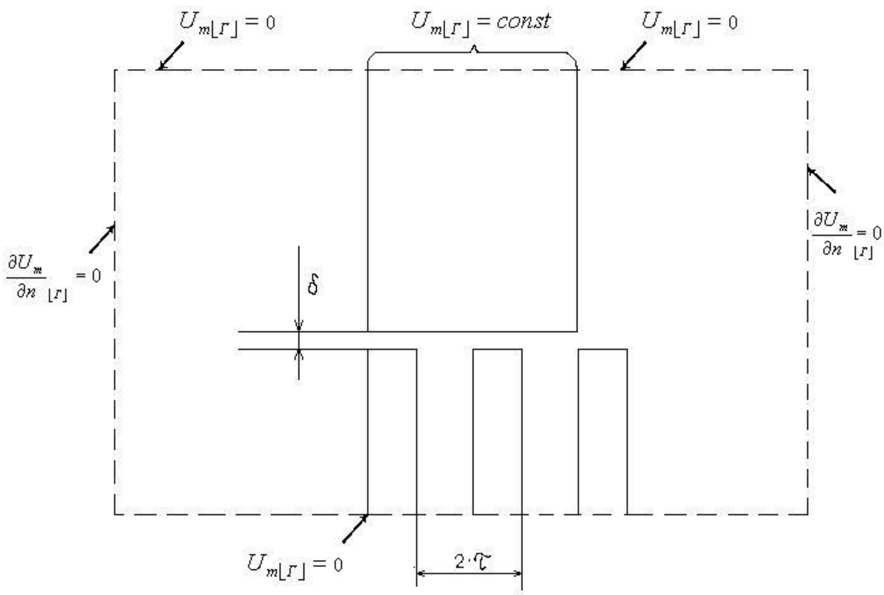

Figure 3

Research area of the magnetic field

3 Results of Simulation Studies

3.1 Geometrical Parameters Impact on Machine Performance

Curves of induction distribution, which have been obtained as a result of computational simulation of field in the air gap (the rotor tooth shape is assumed to be rectangular), are shown in Fig. 4.

Simulation of the magnetic field parameters in an electric machine in order to find out the qualitative and quantitative evaluation of the induction distribution in the air gap also allows to carry out its harmonic analysis.

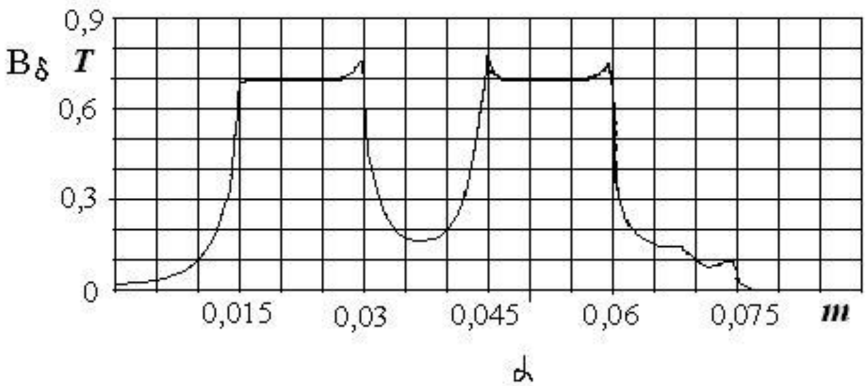

Figure 4
Curve of magnetic induction in the air gap (for rectangular rotor tooth shape)

Variable algorithm of searching the optimum shape of the curve of magnetic induction distribution in the air gap allows to define the following:

- Step-by-step synthesis of the pole shape, as it is shown in Fig. 5;
- Variation of the pole factor $\alpha_{\ddot{I}} = b_p / \tau$,

  where b_P is pole span, m; τ is pole pitch, m.

Estimation method of shape factor K_S of the air gap under stator pole is illustrated by Fig. 5 and relationship given by:

$$K_S = {S_M}/{S_0} .$$

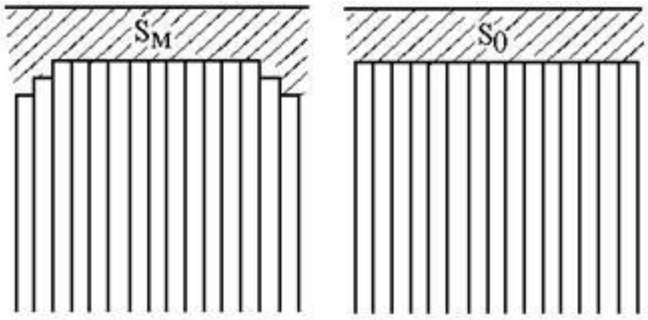

Figure 5
Estimation method of shape factor K_S of the air gap under stator pole

Harmonic composition of the induction distribution curve along the rotor surface is determined by the following factors:

1. Form factor of variable component of the magnetic field of excitation for ν- th harmonic is determined in terms of formula:

$$\hat{E}_{f\nu} = \frac{B_{\delta m\nu}}{B_m},$$

where $B_{\delta m\nu}$ is peak value of the magnetic induction harmonic with number ν in the air gap, T;

B_m is peak value of magnetic induction in the air gap on the axis of the rotor pole, T.

2. Utilization factor of the magnetic field is given by [5]:

$$K_{\grave{e}} = \frac{B_{\delta 1m}}{A(0)/2},$$

where: A(0)/2 is zero harmonic of the magnetic field in the air gap of the machine, T;

$B_{\delta 1m}$ is peak value of first harmonic of magnetic induction in the air gap, T

Based on outcomes of computational simulation the influence of the required factors on the magnetic induction distribution can be estimated to vary the pole shape of the machine. One of the variants of the form factor and the utilization factor subject to geometry of the tooth zone is shown as graphs in Fig. 6-7.

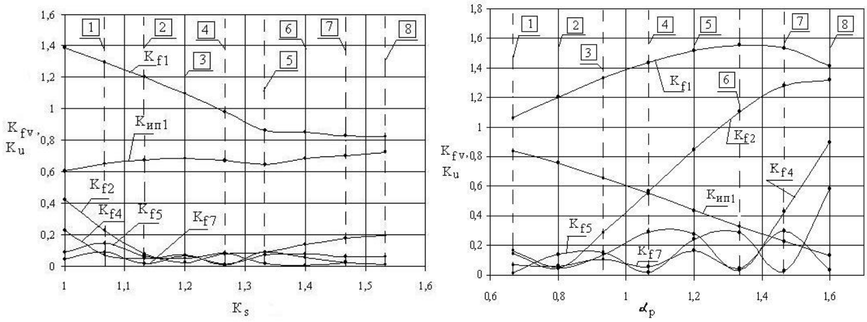

Figure 6

Functions of form factor and the utilization factor subject to geometry of the tooth zone

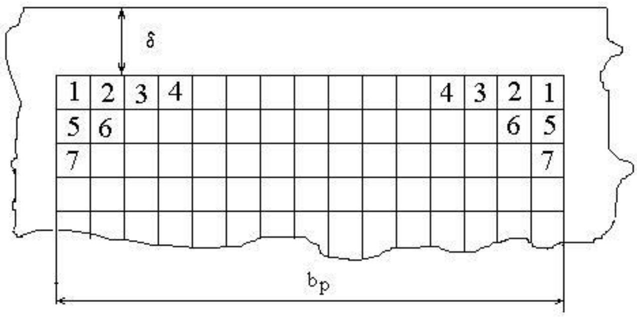

Figure 7

Diagram of shape variation sequence in order, indicated by numbers, in which the pole sheets are cut out

The simulation model study findings have shown significant influence of the air gap value on ripple of the generator magnetic field. Numerical values of ripple factor K_P, subject to air gap, are shown in table 1.

Table 1

Dependance of ripple factor on air gap

Air gap, m.	Ripple factor Kp
0.002	1.1
0.003	1.141
0.004	1.294

3.2 Chamfer Factor Influence on the Generator Operation

Design of the generator, where stator is made up in the form of an arc, has both the rotor tooth zone and stator slots with arc-shape geometry. When the rotor teeth are located radially, the stator slot axes are in parallel [6]. The axial matching of stator and rotor teeth, which are located in the middle of the arc, should be noted. When moving along the rotor tooth axis to the edge of the arc, the slot chamfer angle is increasing (Fig. 8, 9). It means that the slot chamfer angle is not a constant, as in standard ac machines, but a variable that is altered 0 to its maximum value [7]. Hereby the influence of the chamfer on the EMF of the armature winding should be studied.

The study of the dependence of the chamfer factor on fundamental harmonic of magnetic induction shown in Fig. 8 allows to obtain localized zone of permissible ratios between number of poles and pole arc angle for edge slots of stator for $K_C \geq 0,7$.

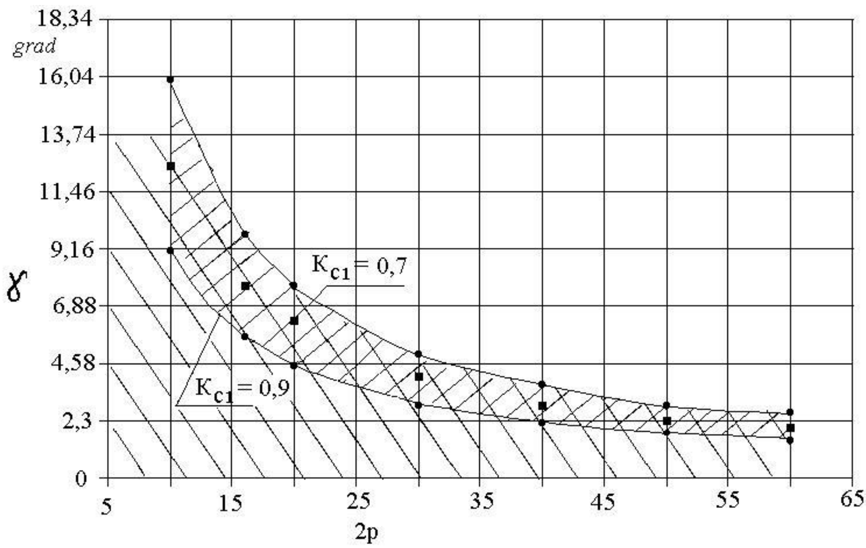

Figure 8

Zone of permissible ratios between number of poles and pole arc angle

EMF $\mathring{A}_q$ of a coil group is determined by adding together the EMF vectors $\Delta\mathring{A}_{\hat{e}}$ of the coils that are shifted in space for angle $\gamma_{\tilde{n}\hat{e}_i}$ (Fig. 10).

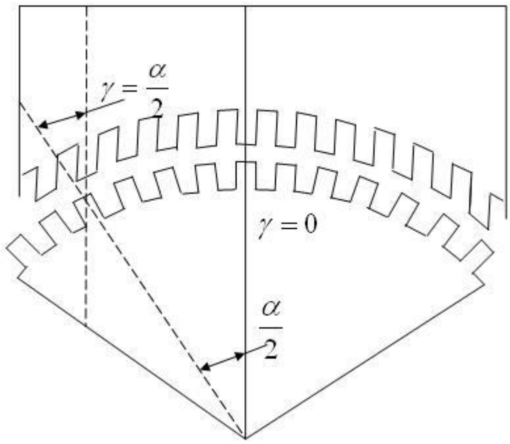

Figure 9

Geometrical interpretation of slot chamfer factor

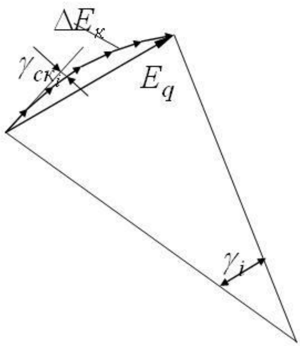

Figure 10

EMF vector of a coil with slot chamfer

Expressions to calculate the slot chamfer factor illustrated by Fig. 9, 10 are given in terms of formulae below:

$$\gamma_{ci} = \frac{\alpha}{2z_i}, \quad 0 \le \gamma_i \le \frac{\alpha}{2}, \quad K_c = \left. \frac{\sin\frac{\alpha}{2}}{\sin\frac{\gamma_i}{2}} \right|_{\gamma_i = \frac{\alpha}{2z_i}}$$

$$K_c = \int_0^{\alpha/2} \frac{\sin\frac{\alpha}{2}}{\sin\frac{\gamma_i}{2}} d\gamma_i = \sin\frac{\alpha}{2} \int_0^{\alpha/2} \frac{dx}{\sin\frac{x}{2}} = 2\sin\frac{\alpha}{2} \int_0^{\alpha/2} \frac{dz}{\sin z}$$

$$K_c = 2\sin\frac{\alpha}{2} \ln\left(\cos ec\, z - ctg\, z\right)\Big|_0^{\frac{\alpha}{2}}$$

The achieved dependences of the slot chamfer factor on chamfer angle are shown in Fig. 11. Approximating function can be specified by 3-rd order poly-nomial determined by:

$$K_{ci} = -0,0607\,\gamma_i^3 - 11,996\,\gamma_i^2 + 0,0039\,\gamma_i + 0,7839.$$

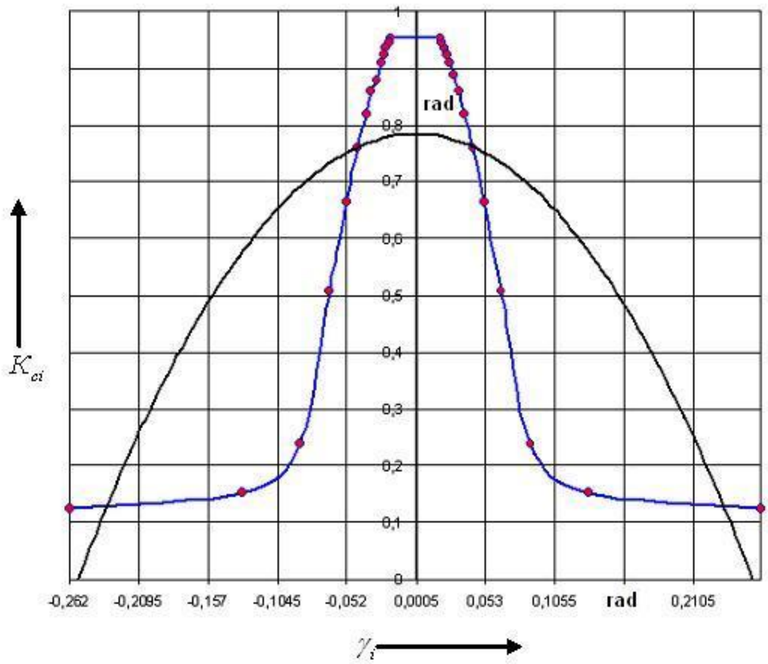

Figure 11

Dependences of the slot chamfer factor K_{ci} on chamfer angle γ_i

Conclusion

Research shows qualitive and quantative influence of design features of an arc-shape stator, rotor poles, geometry parameters of the air gap on spectral composition and power efficiency of the magnetic field. It allows determining optimal range of variation of the slot chamfer and dependence of first harmonic of EMF on it.

Analysis of the obtained calculated and simulation data shows that the generator output parameters (form factor, utilization factor, ripple factor) are influenced by geometrical parameters of the machine. In addition, the impact of the the air gap on the ripple factor is found to be significant.

Functional dependence of the slot chamfer factor on chamfer angle has been found, which simplifies the problem of choosing reasonable, in terms of efficiency, design parameters of the generator of a micro hydropower plant.

Acknowledgments

The research is funded from Tomsk Polytechnic University Competitiveness Enhancement Program grant, Project Number TPU CEP_IPE_97\2017.

References

[1] Müller, G.a , Kauppert, K.b Performance characteristics of water wheels. - Journal of Hydraulic Research. Volume 42, Issue 5, 2004, Pages 451-460.

[2] Anagnostopoulos, J.S. , Papantonis, D.E. Optimal sizing of a run-of-river small hydropower plant. - Energy Conversion and Management. Volume 48, Issue 10, October 2007, Pages 2663-2670.

[3] Müller, G., Denchfield, S., Marth, R., Shelmerdine, R. Stream wheels for applications in shallow and deep water (2007) Proc 32nd IAHR Congress, Venice C (2c, Paper 291).

[4] Generator for micro power plant// V. M. Kuzmin, G. A. Sedov, V. I. Suzdorf /Patent 39918 of Russian Federation, MPK H02P7/29. publ. in bull. №23, 2004 (in Russian).

[5] Suzdorf V.I. Simulation of voltage sources for autonomous power supply system. Education and science: actual state and outlook// Proceedings of conference NTK 31st of July 2014: in 6 vol. Vol.3. Tambov: «Consulting company Yukom», 2014.- p.128-130 (in Russian).

[6] Victor I. Suzdorf, Aleksandr S. Meshkov, Yuri N. Dementyev and Dmitriy A. Kaftasyev Energy efficiency improvement of medical electric tools and devices// The 2nd International Youth Forum “Smart Grids”, MATEC Web of Conferences, Volume 19, 2014. -Published online: 15 December 2014.

[7] Quaranta, E. , Revelli, R. Performance characteristics, power losses and mechanical power estimation for a breastshot water wheel. – Energy. Volume 87, 1 July 2015, Pages 315-325.